

Fermion-Boson Stars as Attractors in Fuzzy Dark Matter and Ideal Gas Dynamics

Iván Alvarez-Rios,^{1,*} Francisco S. Guzmán,^{1,†} and Jens Niemeyer^{2,‡}

¹*Instituto de Física y Matemáticas, Universidad Michoacana de San Nicolás de Hidalgo. Edificio C-3, Cd. Universitaria, 58040 Morelia, Michoacán, México.*

²*Institut für Astrophysik und Geophysik, Georg-August-Universität Göttingen, D-37077 Göttingen, Germany*
(Dated: December 19, 2024)

In the context of Fuzzy Dark Matter (FDM) we study the core formation in the presence of an Ideal Gas (IG). Our analysis is based on the solution of the Schrödinger-Poisson-Euler system of equations that drives the evolution of FDM together with a compressible IG, both coupled through the gravitational potential they produce. Starting from random initial conditions for both FDM and IG, with dominant FDM, we study the evolution of the system until it forms a nearly relaxed, virialized and close to hydrostatic equilibrium core, surrounded by an envelope of the two components. We find that the core corresponds to Newtonian Fermion-Boson Stars (FBS). If the IG is used to model luminous matter, our results indicate that FBS behave as attractor core solutions of structure formation of FDM along with baryonic matter.

Keywords: self-gravitating systems – dark matter – Bose condensates – cosmology

The Fuzzy Dark Matter (FDM) model assumes dark matter is an ultralight boson of masses of order $10^{-23} - 10^{-21}$ eV [1–6]. Among its key predictions allowing an observational distinction from standard cold dark matter (CDM) is the formation of smooth cores that are stabilized against collapse by scalar gradient energy, as demonstrated in simulations of cosmological structure formation [7–12]. Since FDM cores are an essential fingerprint of the model, their formation and relaxation has been studied from different angles, for example, using multi-mergers of cores that eventually merge to form new virialized cores [8, 13–16]. Another approach is to study the kinetic relaxation as the process to condensate cores, since within the Jeans regime, structures condense and grow over time by accreting the ambient FDM [17–21]; in these studies random initial conditions lead to the formation and condensation of a core. In the three methods of core formation it has been found that the core has a density that averaged over the solid angle resembles the density of the ground state solution of the Schrödinger-Poisson system of equations, namely the Newtonian ground state version of a Boson Star [22], later on associated to Bosonic Dark Matter [23], that has attractor properties [24, 25], and whose density profile has been modeled with a universal phenomenological formula [7, 13].

The properties of FDM cores are a crucial ingredient in the efforts to constrain allowed boson masses from galactic rotation curves [26]. Most theoretical studies so far have ignored the presence of baryonic components while hydrodynamic simulations starting from realistic cosmological initial conditions are hampered by resolution requirements. Furthermore, ultrafaint dwarf galaxies offering some of the strongest constraints on the core profile

are believed to be dominated by dark matter. Nevertheless, baryonic luminous matter (LM) was shown to significantly affect the FDM core properties in more massive halos [27], motivating a more general treatment of core formation.

Although LM is not essential for core formation within the FDM model, its inclusion should provide valuable insight about the interactions between dark and baryonic components. LM on the other hand can be modeled as a multi-component gas with a great variety of properties, however a proof of concept model can assume LM is an Ideal Gas (IG) that could provide the starting point to more detailed studies on the interaction between FDM and LM. We start from this assumption in this letter and follow an approach similar to that of kinetic relaxation to study the evolution of random initial conditions of a sea of FDM together with a distribution of IG, aiming to learn whether FDM+IG cores are also formed and what properties these may have. What we find is that cores actually form and these correspond to stationary solutions of the Schrödinger-Poisson-Euler system of equations for an ideal gas and a boson gas in hydrostatic equilibrium. These solutions are the Newtonian version of the so called Fermion-Boson Stars [28], whose construction and stability properties we review in [29]. In this letter we show that these cores, likewise those of pure FDM, are solutions that behave as attractors.

Model. We assume that the dynamics of FDM gravitationally interacting with the IG is governed by the SPE equations, which in Code Units (CU) take the following form [29, 30]:

$$i\partial_t\Psi = -\frac{1}{2}\nabla^2\Psi + V\Psi, \quad (1)$$

$$\partial_t\rho + \nabla \cdot (\rho\vec{v}) = 0, \quad (2)$$

$$\partial_t(\rho\vec{v}) + \nabla \cdot (\rho\vec{v} \otimes \vec{v} + p\mathbf{I}) = -\rho\nabla V, \quad (3)$$

$$\partial_t E + \nabla \cdot [\vec{v}(E + p)] = -\rho\vec{v} \cdot \nabla V, \quad (4)$$

$$\nabla^2 V = \rho + \rho_{FDM}, \quad (5)$$

* ivan.alvarez@umich.mx

† francisco.s.guzman@umich.mx

‡ jens.niemeyer@phys.uni-goettingen.de

where Ψ is the order parameter describing FDM dynamics, $\rho_{FDM} = |\Psi|^2$ is the FDM density, ρ , \vec{v} and p are the mass density, velocity field and pressure of the IG, with total energy given by $E = \rho(e + \frac{1}{2}|\vec{v}|^2)$, where e is the specific internal energy. Notice that V is the gravitational potential generated by the two components and is the only coupling between them. To complete the system, an Equation of State (EoS) for the gas is specified. For this we use two, one is that of an ideal gas:

$$p = (\gamma - 1)\rho e, \quad (6)$$

used for the evolution, and the other one is the polytropic EoS:

$$p = K\rho^{1+1/n}, \quad (7)$$

where γ is the adiabatic index in the ideal gas EoS (6), K and n are the polytropic constant and index given by γ as $\gamma = 1 + 1/n$ in isentropic processes. We use this EoS in the construction of the initial conditions for the IG.

Initial Conditions. For the FDM we follow the approach in [31], which demonstrates that condensation is an inherent feature of the FDM system, in a variety of scenarios independent of the initial shape of the initial cloud [18]. Therefore, the initial condition for the FDM component defines the order parameter in momentum space as $\hat{\Psi}(\vec{p}) = Ae^{-0.5p^2}e^{i\Theta}$, where Θ is a random phase between $[0, 2\pi]$ at each momentum space point, and A is a normalization factor ensuring a total mass M_{FDM} . For the IG we follow a similar strategy, we establish initial conditions for the fluid variables by generating an auxiliary wave function analogous to that of FDM, we then extract the mass density and velocity using the Madelung transformation [32], $\tilde{\Psi} = \sqrt{\rho}e^{i\tilde{S}}$, where the velocity \vec{v} is defined as $\nabla\tilde{S}$; finally we set the initial pressure using the polytropic EoS (7), and calculate the initial specific internal energy using Eq. (6).

In the cosmological context, this setup can be interpreted as an idealized homogeneous ensemble of density and velocity fluctuations formed during the violent relaxation of a collapsed halo. The free parameters γ and K characterizing the IG offer a well-posed approach to study the sensitivity of the final configuration to the properties of the multi-phase galactic ISM. More complex behavior, such as density-dependent cooling or kinetic feedback, is not expected to change our qualitative results but will have to be included for quantitative predictions. This is left for future work.

Parameter Space. We use the adiabatic index for a monatomic gas set to $\gamma = 5/3$, which corresponds to a polytropic index of $n = 3/2$ for isentropic processes. Because specific internal energy is proportional to temperature, and in this case, also to the polytropic constant K , we explore temperature effects of the IG at initial time, by setting K to values of 0.1, 1, and 10 in Code Units. The FDM mass is fixed to $M_{FDM} = 1005.3$ in a

cubic domain of size $L = 18$, parameters we take from an independent standard core formation simulation [18]. We define the mass of the IG component through a mass ratio $M_{IG} = MR \cdot M_{FDM}$, and use $MR = 0.1$ and 0.2 .

Simulations Setup. The simulations are performed with our code CAFE-FDM described and tested in [15, 33]. For the purposes of this letter, we use a third-order Runge-Kutta (RK3) scheme for time integration and impose periodic boundary conditions to all variables. The right-hand side of Schrödinger equation (1) is discretized using the Fast Fourier Transform (FFT), while Euler equations (2)-(4) are solved with High-Resolution Shock-Capturing methods, specifically with the HLLE flux formula and the minmod limiter for variable reconstruction. Poisson equation is solved at each RK3 step using the FFT method. The spatial domain is a cube discretized with $N = 128$ grid points along each dimension, using spatial resolution of $h = L/128 = 9/64$. The time step is set to satisfy the Courant condition $\Delta t/h^2 < \frac{1}{6\pi}$, as recommended in [18], and finally the SPE system is closed with the ideal gas EoS (6) during the evolution.

Evolution. The evolution of FDM and gas densities is illustrated for the simulations with $MR = 0.1$ in Fig. 1, with snapshots taken at times $t = 0, 7, 14, 50,$ and 100 , from left to right in each column; each row corresponds to different initial polytropic constant $K = 0.1, 1.0,$ and 10 , respectively. The FDM density is described with the color map, while the isocontours indicate the IG distribution. These plots reveal that FDM condensation drives the collapse of the IG component, indicating that the initial mixture of FDM-IG starting from an initially random distribution of these two matter components leads to a final collapse. FDM is known to condense into a stable configuration that, on average, aligns with the ground state of the Schrödinger-Poisson system [15, 31], and this behavior leads the IG to condensate, following the gravitational potential of the FDM core, a Boson Star in formation [18]. To further analyze this behavior, we present additional diagnostics below.

Diagnostics. The evolution reveals that the matter distribution condenses into a nearly stable configuration. To investigate this in more detail, we compute an angularly average density over the solid angle $\Omega = [0, \pi] \times [0, 2\pi]$ given by $f_{\text{avg}} = \frac{1}{4\pi} \int_{\Omega} f d\Omega$ that we use to calculate averaged densities, in our case f will be ρ_{FDM} and ρ . Fig. 2 presents the angularly averaged densities of the FDM and IG components for the simulations with $MR = 0.1$, while similar results are found for $MR = 0.2$. Each row corresponds to averages calculated at times $t = 0, 7, 14, 50,$ and 100 . The red solid, blue dashed, and black dotted lines correspond to the polytropic constants $K = 0.1, 1,$ and 10 , respectively, used at initial time. The FDM forms a solitonic core surrounded by an extended tail, while the IG component shows that, after 14 time units, its density profile becomes more compact as K is smaller. This behavior suggests that higher initial temperatures result in a lower central density of the final configuration.

The evolution of the condensation, at least that of the

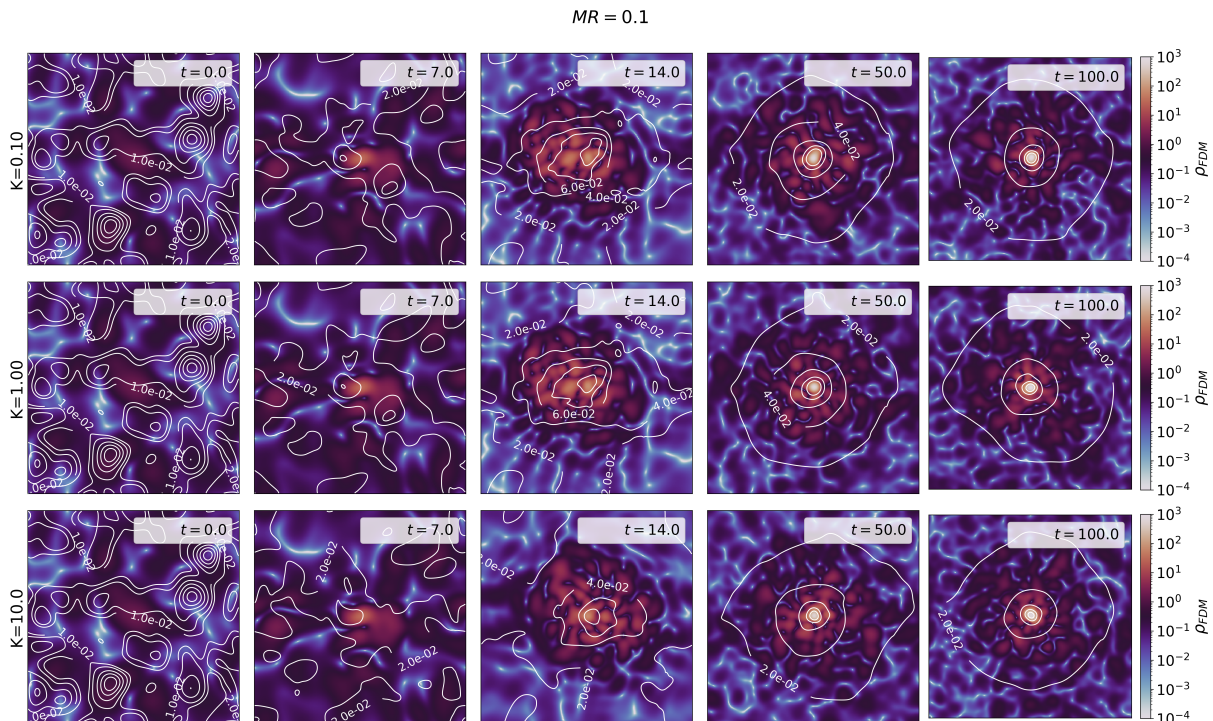


FIG. 1. Evolution of ρ_{FDM} and ρ densities for the simulations with $MR = 0.1$, described by color maps and isocontours respectively. These plots are centered at the maximum of the FDM density for ease of illustration. Each column presents snapshots at times $t = 0, 7, 14, 50$, and 100 , while each row corresponds to simulations with polytropic constants $K = 0.1, 1.0$, and 10 . Similar results are found for $MR = 0.2$.

FDM as indicated in [18, 31], can be followed through the maximum of the density that reveals how the core accretes mass from the surroundings until saturation. In Fig. 3 we show the maximum of ρ_{FDM} and ρ as function of time, for the two values of $MR = 0.1, 0.2$ and the three values of $K = 0.1, 1, 10$. Blue solid lines and orange dashed lines represent the results for $MR = 0.1$ and $MR = 0.2$. In all cases, the maximum of ρ_{FDM} grows as typically without the IG starting at condensation time τ_g [18, 31], in our case $\tau_g \sim 7$, and from then on the condensation of a core starts happening. On the other hand, the density of the IG prior to τ_g is erratic and in fact decreases, which indicates a stage of nearly uniform distribution, however, after τ_g the IG density grows and stabilizes, which indicates that after the FDM starts condensing and its dominating gravitational potential gets deeper, the IG starts accumulating around there and stabilizes. This is confirmed by the snapshots in Fig. 1.

The condensation process results in an FDM-IG core that settles into a virialized configuration of the Schrödinger-Poisson-Euler (SPE) system as shown next. Fig. 4 shows the evolution of the various energies involved for the simulations with $MR = 0.1$. For the FDM component these energies include the kinetic energy $K_{FDM} = -\frac{1}{2} \int_D \Psi^* \nabla^2 \Psi d^3x$, the gravitational energy $W_{FDM} = \frac{1}{2} \int_D |\Psi|^2 V d^3x$, the total energy $E_{FDM} = K_{FDM} + W_{FDM}$, and the virial factor $Q_{FDM} = 2K_{FDM} +$

W_{FDM} . For the gas component, the scalars are the kinetic energy $K_{IG} = \frac{1}{2} \int_D \rho |\vec{v}|^2 d^3x$, the gravitational energy $W_{IG} = \frac{1}{2} \int_D \rho V d^3x$, the internal energy $U_{IG} = \int_D \rho e d^3x$, the total energy $E_{IG} = K_{IG} + W_{IG} + U_{IG}$, and the virial factor $Q_{IG} = 2K_{IG} + W_{IG} + 3U_{IG}$. Similar results are found for the simulations with $MR = 0.2$.

The plots illustrate two key aspects of the evolution. First, the virial factor $Q = Q_{FDM} + Q_{IG} \approx 0$ for times $t > \tau_g$ indicates that the system has approached a dynamically stable equilibrium. This near-zero value of Q is a reliable indicator of virialization. As a result, the overall structure no longer undergoes significant changes, indicating that the system has settled around stable configuration.

A second lead is the decrease of the IG kinetic energy toward zero, which indicates not only the approach toward a stationary state but also the approach toward hydrostatic equilibrium. In hydrostatic equilibrium, the inward gravitational force is balanced by the outward pressure forces, resulting in a configuration stable against both collapse and expansion. The small kinetic energy suggests minimal bulk motion within the gas, indicating that the gas distribution has settled into a nearly steady-state configuration. Consequently, this relaxed configuration of FDM-IG, formed through the condensation process, transitions to a structure that maintains equilibrium under its self-gravity and pressure forces, which are characteristics of a self-gravitating, hydrostatically balanced

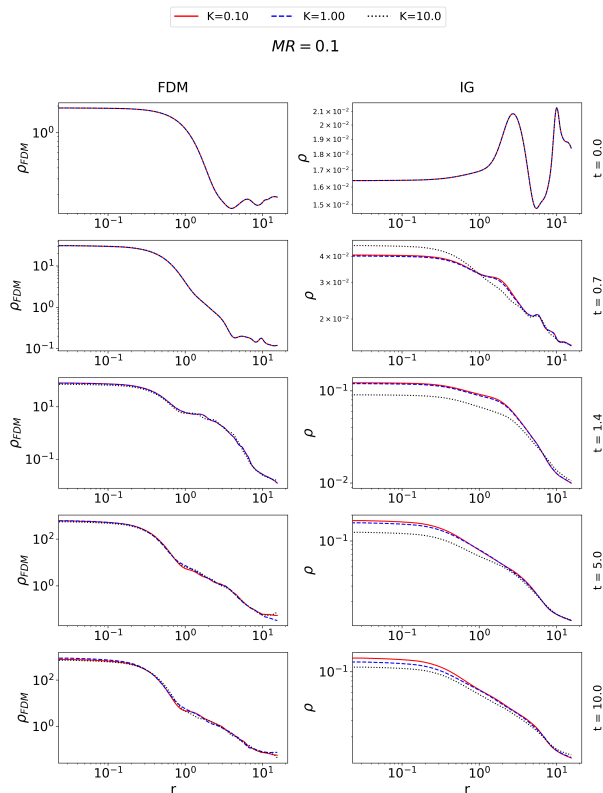


FIG. 2. Angularly averaged ρ_{FDM} and ρ at various times centered at the maximum of ρ_{FDM} for the simulations with $MR = 0.1$. The red solid line, blue dashed line, and black dotted line correspond to initial values of $K = 0.1$, 1 , and 10 , respectively. Similar results are found for $MR = 0.2$.

stationary Newtonian FBS [29].

In Fig. 5 we compare the angularly averaged ρ_{FDM} and ρ after relaxation, with the densities of a ground state solution of a Newtonian FBS for one of our simulations with $MR = 0.1$ at time $t = 100$. An additional information of FBS is that they are constructed assuming a polytropic EoS, and in the case of Fig. 5, the FBS that fits the densities has a polytropic constant ~ 103.5 . This type of fitting suggests not only that the FDM-IG system reaches radial-hydrostatic equilibrium, but also that entropy is nearly conserved, highlighting the robustness of these solutions.

Concerning the properties of the final configurations, the results can be summarized as follows. For a given MR , the central density and core radius of the FDM is independent of the initial polytropic constant K of the IG within a few percent; on the other hand, for the IG we find that for the bigger K , the central density is smaller, indicating that the bigger the K , the less compact the IG distribution within the FDM core. This diversity of FDM and IG distributions are contained within wide range of FBS solutions [29].

Conclusions. The condensation of the dominant FDM induces the stabilization of the IG, driving the system toward a virialized state. The system evolves into a dy-

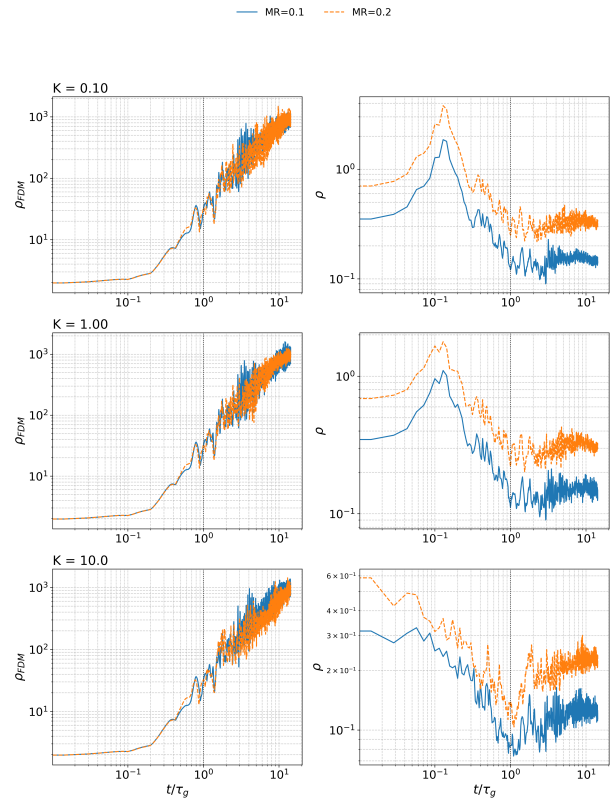


FIG. 3. Maximum of ρ_{FDM} (left) and ρ (right) as function of time. Top, middle and bottom rows correspond to initial polytropic constants $K = 0.1$, 1 , and 10 . Blue solid and orange dashed lines indicate the cases with mass ratios $MR = 0.1$ and $MR = 0.2$.

namically stable equilibrium, characterized by a virial factor $Q \approx 0$ and a reduction in the kinetic energy of the gas, suggesting hydrostatic equilibrium. This indicates that the system stabilizes under its own self-gravity and pressure forces, transitioning from an initial blob formed from random initial conditions, into a stationary configuration of the SPE system. The results show the formation of a FBS from an initially random distribution of FDM and an IG with an 80% and 90% of FDM mass, and could be extended to study the formation and phenomenology of FBS in scenarios where the IG dominates.

In the context of FDM, if the IG is to be considered as a simple model of luminous matter, the attractor nature of FBS would imply that the distribution of the IG associated to luminous matter, should be common in galactic cores. In this sense, FBS as cores can impose limitations to the FDM model. One alternative can be the study of the coupling of oscillations between the two components, that has been found happen for FBS [29].

The attractor character of FBS can be further explored by examining dynamical evolutions from smooth initial conditions, such as spherical collapse models. Moreover, non-ideal gas properties of the ISM can be studied by adding cooling and heating terms to Eq. (4). This will provide crucial improvements to FDM halo models used

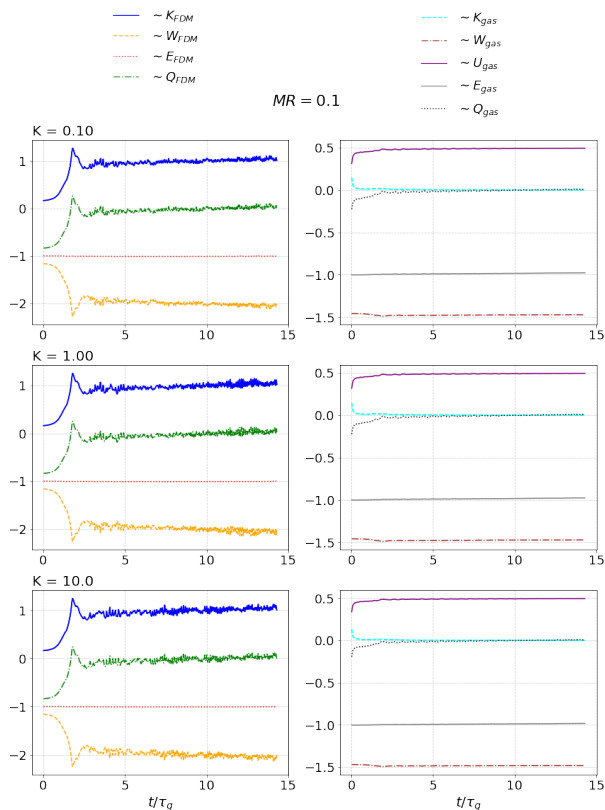


FIG. 4. Time evolution of the FDM and IG properties as function of time for the simulations with $MR = 0.1$. These plots illustrate the virialization process of the FDM-IG system, that leads to the formation of a Newtonian FBS. For the FDM component, we show the kinetic energy K_{FDM} , gravitational energy W_{FDM} , total energy E_{FDM} , and the virial factor Q_{FDM} , all normalized by the initial absolute total energy $|E_{\text{FDM}}(0)|$. For the IG component, we display the kinetic energy K_{IG} , gravitational energy W_{IG} , internal energy U_{IG} , total energy E_{IG} , and the virial factor Q_{IG} , each one normalized by the initial absolute total energy $|E_{\text{IG}}(0)|$. These energy diagnostics emphasize the stabilization of the system into a virialized configuration, with both FDM and IG components achieving distinct but stable energy values over time. Finally $Q_{\text{FDM}} \sim 0$ and $Q_{\text{IG}} \sim 0$ with time, which indicates that the two components evolve near a virialized state separately. Similar results are found for $MR = 0.2$.

in precision constraints on allowed boson masses [34].

Thinking beyond the FDM-IG attractor cores, other scenarios offer more freedom to obtain less symmetric configurations of FDM+IG based on interaction between various structures, for example spiral, disk and bullet-shaped contours of IG can be constructed [30], which may provide the sufficient variety of observed luminous structures beyond FBS cores but within the FDM phenomenology.

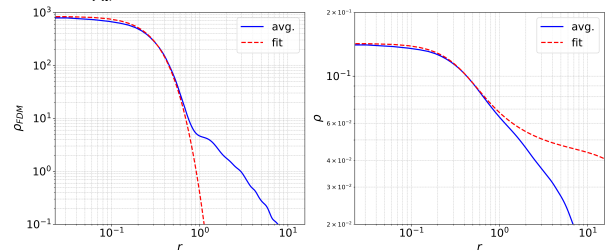


FIG. 5. Angular average of ρ_{FDM} at the left and ρ at the right for the case $MR = 0.1$, $K = 0.1$ at time $t = 100$ when the core has relaxed. These densities in the core are compared with the densities of a Newtonian FBS. Keeping in mind that FBS are constructed using a polytropic EoS [29], we find that the FBS that fits these relaxed densities of the FDM-IG core has a polytropic constant ~ 103.5 . These results indicate that the FDM-IG core approaches a stable FBS, with radial-hydrostatic equilibrium and entropy nearly conserved, supporting the attractor nature of FBS. All other simulations have similar fits. For this type of fitting we do not use a phenomenological universal formula describing the densities, instead we solve the eigenvalue problem of FBS many times and search the fitting parameters using a Genetic Algorithm.

ACKNOWLEDGMENTS

Iván Álvarez receives support from the CONAHCyT graduate scholarship program. This research is supported by grants CIC-UMSNH-4.9, Laboratorio Nacional de Cómputo de Alto Desempeño Grant No. 1-2024, CONAHCyT Ciencia de Frontera 2019 Grant No. Sinergias/304001.

-
- [1] Wayne Hu, Rennan Barkana, and Andrei Gruzinov, “Cold and fuzzy dark matter,” *Phys. Rev. Lett.* **85**, 1158–1161 (2000).
 - [2] Pierre-Henri Chavanis, “Self-gravitating bose-einstein condensates,” in *Quantum Aspects of Black Holes*, edited by Xavier Calmet (Springer International Publishing, Cham, 2015) pp. 151–194.
 - [3] Lam Hui, Jeremiah P. Ostriker, Scott Tremaine, and Edward Witten, “Ultralight scalars as cosmological dark matter,” *Phys. Rev. D* **95**, 043541 (2017).
 - [4] Jens C. Niemeyer, “Small-scale structure of fuzzy and axion-like dark matter,” *Progress in Particle and Nuclear Physics* **113**, 103787 (2020).
 - [5] Lam Hui, “Wave dark matter,” *Annual Review of Astronomy and Astrophysics* **59**, 247–289 (2021).
 - [6] Elisa G. M. Ferreira, “Ultra-Light Dark Matter,” arXiv e-prints, arXiv:2005.03254 (2020), arXiv:2005.03254 [astro-ph.CO].
 - [7] Hsi-Yu Schive, Tzihong Chiueh, and Tom Broadhurst, “Cosmic Structure as the Quantum Interference of a Coherent Dark Wave,” *Nature Phys.* **10**, 496–499 (2014a), arXiv:1406.6586 [astro-ph.GA].
 - [8] Philip Mocz, Mark Vogelsberger, Victor H. Robles, Jesús Zavala, Michael Boylan-Kolchin, Anastasia Fialkov, and

- Lars Hernquist, “Galaxy formation with Λ CDM I. turbulence and relaxation of idealized haloes,” *Mon. Not. Roy. Astron. Soc.* **471**, 4559–4570 (2017), [arXiv:1705.05845 \[astro-ph.CO\]](#).
- [9] Jan Veltmaat, Jens C. Niemeyer, and Bodo Schwabe, “Formation and structure of ultralight bosonic dark matter halos,” *Physical Review D* **98** (2018), [10.1103/physrevd.98.043509](#).
- [10] Philip Mocz, Anastasia Fialkov, Mark Vogelsberger, Fernando Becerra, Mustafa A. Amin, Sownak Bose, Michael Boylan-Kolchin, Pierre-Henri Chavanis, Lars Hernquist, Lachlan Lancaster, Federico Marinacci, Victor H. Robles, and Jesús Zavala, “First star-forming structures in fuzzy cosmic filaments,” *Phys. Rev. Lett.* **123**, 141301 (2019).
- [11] Simon May and Volker Springel, “Structure formation in large-volume cosmological simulations of fuzzy dark matter: impact of the non-linear dynamics,” *Monthly Notices of the Royal Astronomical Society* **506**, 2603–2618 (2021).
- [12] Bodo Schwabe and Jens C. Niemeyer, “Deep zoom-in simulation of a fuzzy dark matter galactic halo,” *Phys. Rev. Lett.* **128**, 181301 (2022).
- [13] Hsi-Yu Schive, Ming-Hsuan Liao, Tak-Pong Woo, Shing-Kwong Wong, Tzihong Chiueh, Tom Broadhurst, and W. Y. Pauchy Hwang, “Understanding the Core-Halo Relation of Quantum Wave Dark Matter from 3D Simulations,” *Phys. Rev. Lett.* **113**, 261302 (2014), [arXiv:1407.7762 \[astro-ph.GA\]](#).
- [14] Bodo Schwabe, Jens C. Niemeyer, and Jan F. Engels, “Simulations of solitonic core mergers in ultralight axion dark matter cosmologies,” *Phys. Rev. D* **94**, 043513 (2016), [arXiv:1606.05151 \[astro-ph.CO\]](#).
- [15] Iván Álvarez-Ríos, Francisco S. Guzmán, and Paul R. Shapiro, “Effect of boundary conditions on structure formation in fuzzy dark matter,” *Phys. Rev. D* **107**, 123524 (2023).
- [16] Iván Álvarez-Ríos and F. S. Guzmán, “Effects of boundary conditions on the core-halo mass scaling relation of fuzzy dark matter structures,” *Phys. Rev. D* **110**, 023530 (2024).
- [17] Benedikt Eggemeier and Jens C. Niemeyer, “Formation and mass growth of axion stars in axion miniclusters,” *Phys. Rev. D* **100**, 063528 (2019).
- [18] Jiajun Chen, Xiaolong Du, Erik W. Lentz, David J. E. Marsh, and Jens C. Niemeyer, “New insights into the formation and growth of boson stars in dark matter halos,” *Phys. Rev. D* **104**, 083022 (2021).
- [19] Jiajun Chen, Xiaolong Du, Mingzhen Zhou, Andrew Benson, and David J. E. Marsh, “Gravitational bose-einstein condensation of vector or hidden photon dark matter,” *Phys. Rev. D* **108**, 083021 (2023).
- [20] Kuldeep J. Purohit, Pravin Kumar Natwariya, Jitesh R. Bhatt, and Prashant K. Mehta, “Formation of a bose star in a rotating cloud,” *Astrophysics and Space Science* **368** (2023), [10.1007/s10509-023-04253-8](#).
- [21] Jiajun Chen and Hong-Yi Zhang, “Novel structures and collapse of solitons in nonminimally gravitating dark matter halos,” *Journal of Cosmology and Astroparticle Physics* **2024**, 005 (2024).
- [22] R. Ruffini and S. Bonazzola, “Systems of self-gravitating particles in general relativity and the concept of an equation of state,” *Phys. Rev.* **187**, 1767–1783 (1969).
- [23] F. S. Guzmán and L. Arturo Ureña López, “Evolution of the schrödinger-newton system for a self-gravitating scalar field,” *Phys. Rev. D* **69**, 124033 (2004).
- [24] F. S. Guzmán and L. Arturo Ureña López, “Gravitational cooling of self-gravitating bose condensates,” *The Astrophysical Journal* **645**, 814–819 (2006).
- [25] Argelia Bernal and F. S. Guzmán, “Scalar field dark matter: Nonspherical collapse and late-time behavior,” *Physical Review D* **74** (2006), [10.1103/physrevd.74.063504](#).
- [26] Nitsan Bar, Kfir Blum, and Chen Sun, “Galactic rotation curves versus ultralight dark matter: A systematic comparison with SPARC data,” *Phys. Rev. D* **105**, 083015 (2022), [arXiv:2111.03070 \[hep-ph\]](#).
- [27] Jan Veltmaat, Bodo Schwabe, and Jens C. Niemeyer, “Baryon-driven growth of solitonic cores in fuzzy dark matter halos,” *Phys. Rev. D* **101**, 083518 (2020), [arXiv:1911.09614 \[astro-ph.CO\]](#).
- [28] Steven L. Liebling and Carlos Palenzuela, “Dynamical boson stars,” *Living Reviews in Relativity* **26** (2023), [10.1007/s41114-023-00043-4](#).
- [29] Iván Álvarez Ríos and Francisco S. Guzmán, “Stationary solutions of the schrödinger-poisson-euler system and their stability,” *Physics Letters B* **843**, 137984 (2023).
- [30] Iván Álvarez-Ríos and Francisco S. Guzmán, “Exploration of simple scenarios involving fuzzy dark matter cores and gas at local scales,” *Monthly Notices of the Royal Astronomical Society* **518**, 3838–3849 (2022).
- [31] D. G. Levkov, A. G. Panin, and I. I. Tkachev, “Gravitational bose-einstein condensation in the kinetic regime,” *Phys. Rev. Lett.* **121**, 151301 (2018).
- [32] Iván Álvarez-Ríos and Francisco S. Guzmán, “Construction and Evolution of Equilibrium Configurations of the Schrödinger–Poisson System in the Madelung Frame,” *Universe* **8**, 432 (2022), [arXiv:2210.15608 \[gr-qc\]](#).
- [33] Iván Álvarez-Ríos and Francisco S. Guzmán, “Exploration of simple scenarios involving fuzzy dark matter cores and gas at local scales,” *Monthly Notices of the Royal Astronomical Society* **518**, 3838–3849 (2022).
- [34] Sophie M. L. Vogt, David J. E. Marsh, and Alex Laguë, “Improved mixed dark matter halo model for ultralight axions,” *Phys. Rev. D* **107**, 063526 (2023), [arXiv:2209.13445 \[astro-ph.CO\]](#).